ELSEVIER

Novel architecture of composite electrode for optimization of lithium battery performance

D. Guy [a], B. Lestriez [a,*], R. Bouchet [b], V. Gaudefroy [a], D. Guyomard [a]

[a] *Laboratoire de Chimie des Solides, Institut des Materiaux Jean Rouxel, CNRS, Université de Nantes, B.P. 32229, 44322 Nantes Cedex 3, France*
[b] *Laboratoire Madirel, Université de Marseille, Centre Sr Jérome, Av. Escadrille Normandie Niemen, 13397 Marseille Cedex 20, France*

Abstract

We show that the polymeric binder of the composite electrode may have an important role on the lithium trivanadate $Li_{1.2}V_3O_8$ electrode performance. We describe a new tailored polymeric binder combination with controlled polymer–filler (carbon black) interactions that allows the preparation of new and more efficient electrode architecture. Using this polymeric binder, composite electrodes based on $Li_{1.2}V_3O_8$ display a room temperature cycling capacity of 280 mAh g^{-1} (C/5 rate, 3.3–2 V) instead of 150 mAh g^{-1} using a standard-type (poly(vinylidene fluoride)–hexafluoropropylene (PVdF–HFP) binder) composite electrode. We have coupled scanning electron microscopy (SEM) observations, galvanostatic cycling and electrochemical impedance spectroscopy in order to define and understand the impact of the microstructure of the composite electrode on its electrochemical performance. Derived from these studies, the main key factors that provide efficient charge carrier collection within the composite electrode complex medium are discussed.
© 2005 Elsevier B.V. All rights reserved.

Keywords: Polymer binder; Carbon black; Composite electrode; Lithium electrode; Lithium trivanadate

1. Introduction

Polymers are mostly studied for their application as the electrolyte solvent of lithium batteries [1], rather than for their application as the binder of composite electrodes. As a result, for composite electrodes in liquid or gelled electrolyte, the binder used is almost systematically poly(tetrafluoro ethylene) (PTFE) or poly(vinylidene fluoride) (PVdF) based polymers. Remarkable improvement resulted however from the use of a copolymer of vinylidene fluoride with hexafluoropropylene (PVdF–HFP) in both electrolyte and composite electrode, which lead to the well-known LiPLIon^{TM} technology [2]. Only very few recent papers give examples of composite electrodes made with other polymers [3–6]. Main goals were to achieve a higher liquid electrolyte uptake by selecting less crystalline polymers thus leading to larger ionic conductivity, or to decrease capacity fading with chemically

more stable polymers. In fact, little is known on the exact role of the polymer binder on composite electrode performance and we think there is a need for fundamental researches on model systems.

This study focuses on the polymeric binder used for lithium trivanadate ($Li_{1.2}V_3O_8$) based composite electrodes, and its influence on the battery performance. $Li_{1.2}V_3O_8$ that offers a theoretical capacity of 360 mAh g^{-1}, was investigated as a very promising positive electrode material during the past two decades [7–10]. However, the experimental capacity generally remains much lower than the theoretical value. It is actually of only 150 mAh g^{-1} with standard-type (PVdF–HFP binder) composite electrode. In this paper, the Li insertion and cycling behaviors of a given $Li_{1.2}V_3O_8$ compound are studied in the same experimental conditions when varying only the polymeric binder of the composite electrode.

Our approach to tailor new polymeric binders is detailed in references [11,12]. Carbon black (CB) has a weak self-ability to form a conductive network around active material particles, which is detrimental to the obtained capacity [13,14].

* Corresponding author. Tel.: +33 2 40 37 39 32; fax: +33 2 40 37 39 95.
E-mail address: Bernard.Lestriez@cnrs-imn.fr (B. Lestriez).

Good polymer–filler interactions are needed to obtain homogeneous dispersion of colloidal CB powder into a polymer matrix, either in the melt or in solution [15,16]. Assuming that such a concept could prevail also for composite electrodes, we selected polyethylene oxide (PEO) that is known to display good polymer–filler interactions with carbon black [17]. We added a plasticizer to increase PEO polymer–filler interactions with carbon black to an excellent level [18]. We also combined plastified PEO with PVdF–HFP. Finally, the liquid electrolyte itself was used as a plasticizer. It is important to emphasize that generally the electrode binder is post-plastified by the electrolyte solvent after activation or assemblage of the battery. In present work, we use a pre-plastification of the composite electrode during electrode fabrication.

2. Experimental

A home-synthesized $Li_{1.2}V_3O_8$ (at 580 °C [19]) was used as the active material, and carbon black (Super-P, noted CB), as a conductive agent. The binders were pure polyethylene oxide, plastified PEO and a plastified polymeric blend of PEO and PVdF–HFP. A mixture of ethylene carbonate (EC)/propylene carbonate (PC) (1:1, w/w) was used as the plasticizer. Battery-grade chemicals such as EC (Merck), PC (Merck), acrylonitrile (Aldrich) and lithium bistrifluorosulfonimide (LiTFSI) were all used as received. PVdF–HFP (Kynar 2801: HFP content 12 wt.%, Atochem) and PEO ($M_w = 300,000$ g mol^{-1}, Solvay) were dried under vacuum at 50 °C for two days before use.

The composite positive electrodes were prepared by following a classical solvent route where acrylonitrile was used as the dispersing medium. The $Li_{1.2}V_3O_8$ and CB powders were dispersed in the binder solution using a roller bank for 12 h in order to form a slurry. For some preparations, liquid electrolyte could also be added at this step. The slurry was further mixed for one day and was then spread on aluminum disks (1 cm^2). These disks were dried at room temperature for 2 h to evaporate the solvent, dried further under vacuum at 50 °C for 1 h, and then, transferred under dry argon atmosphere in a glove box (H$_2$O < 1 ppm) for battery assembly. For comparison, PVdF–HFP based standard composite electrodes were prepared using cyclopentanone as the dispersing medium. In all cases the mass loading was about 4–5 mg of active material per cm^2.

Two-electrode Swagelok™ test cells [20] using the composite positive electrodes, a porous paper soaked with the electrolyte as the separator, and metallic lithium as the negative electrode, were assembled in the glove box. A mixture of EC/PC (1:1, w/w) containing 1 M LiTFSI was used as liquid electrolyte. All voltages given in the text are reported versus Li$^+$/Li. Cell cycling was performed at 20 °C, monitored by a VMP™ system in galvanostatic mode. The voltage range used was 3.3–2 V. All composite electrodes were studied with the same current rate, calculated by considering that the inser-
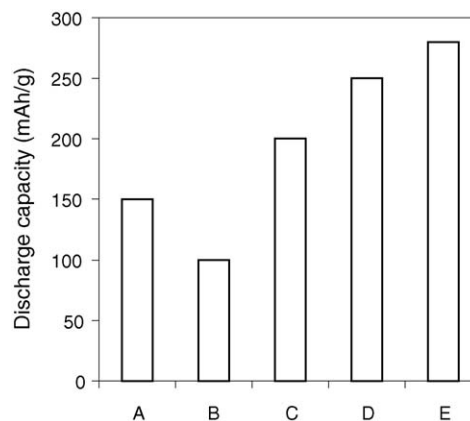

Fig. 1. Electrochemical data. Discharge capacity at room temperature for different cells made with composite electrodes A–E. The experimental discharge rates are: (A) *C*/4, (B) *C*/3, (C) *C*/5, (D) *C*/6 and (E) *C*/7.

tion of one lithium per formula unit lasted 2.5 h in discharge and 5 h in charge. The resulting discharge duration is given by *n* (in hours) in *C/n* in the caption of Fig. 1.

Two-electrode measurements of the electronic conductivity were performed by sandwiching disks of composite tapes between current collectors under an applied pressure of 17 MPa. The impedance of the samples was measured at 25 °C by means of a frequency response analyzer (Solartron 1260) in the 1 Hz–200 kHz frequency range. In these experimental conditions, the electronic conductivity of carbon black alone was measured to be 10 S cm^{-1}. Scanning electron microscopy (SEM) imaging was performed on gold–palladium sputtered samples using a JEOL JSM 6400F apparatus.

3. Results and discussion

The composition of the composite electrodes studied in this paper is given in Table 1. Electrochemical performance of composites A–E is shown in Fig. 1. For these electrodes made with the same $Li_{1.2}V_3O_8$ active material and the same CB, cycling performance considerably changes with the nature of the binder. For the standard composite A, a constant cycling capacity of 150 mAh g^{-1} was displayed. Composite B whose binder is PEO, showed a stable discharge capacity of 100 mAh g^{-1}. Adding the plasticizer produced a net increase of cycle performance. Indeed, for composite C whose binder is plastified PEO, a constant cycling capacity of 200 mAh g^{-1} was displayed. Better performance was obtained for a mixed binder of plastified PEO/PVDF–HFP blend. For this composite D, the cycling performance was 250 mAh g^{-1}. Finally, optimum performance was displayed by composite E where the liquid electrolyte EC–PC LiTFSI (1 M) was used as the plasticizer. The discharge capacity remained stable upon cycling at 280 mAh g^{-1}. This electrode even allowed reaching the theoretical capacity 330 mAh g^{-1} either at low rate (*C*/200) or at 55 °C. The different capacity data readily come

Table 1
Composition of the composite electrodes before battery assembly

Material	DM composition: weight percentage				L: $\alpha\%$	
	$Li_{1.2}V_3O_8$	CB	PVdF–HFP	PEO	EC–PC	EC–PC LiTFSI 1 M
A	85	10	5			
B	54	14	–	32	–	–
C	54	14	–	32	13.6	–
D	54	14	16	16	22.0	–
E	54	14	16	16	–	27.8

The dry matter (DM) composition is explained for clarity. In case of $\alpha\%$ liquid (L) additive (plasticizer or electrolyte), the electrode composition is $(1 - \alpha)DM + \alpha L$.

from a different environment of the active material within the composite electrode, and they are not due to differences in cycling rates. As a matter of fact, the power dependence of most composite electrodes has been studied (not reported here) and shows that the capacity variation for each electrode within the range $C/3–C/7$ is much lower than the capacity variation observed here when changing the binder. Several characterization techniques have been combined in order to shed some light on the origin of the performance improvement.

SEM observation of the surface of composite electrodes has been performed, and results are reported for composite E on Fig. 2. A systematic observation of the morphology of separate components of the composite electrode helped to provide the interpretation [11]. As a summary, the PEO/CB and PEO/CB/plasticizer mixtures form dense homogeneous paste of CB aggregates, which connects the $Li_{1.2}V_3O_8$ flat sticks (composites B and C). PVdF–HFP when processed in room temperature acrylonitrile appears as poorly plastified isolated spheres and/or aggregates of spheres. When a combination of PEO/PVdF–HFP/CB/plasticizer mixture is used (composites D and E), the poorly plastified PVdF–HFP spheres are dispersed in a continuous 3D network of PEO/CB/plasticizer connecting the $Li_{1.2}V_3O_8$ grains together (see Fig. 2). No difference in the morphology of composites D and E was detected. Porosity was roughly independent of the composition and around 70% for electrodes B–E [12]. This value is slightly higher but comparable to what has been measured for calendared $LiMn_2O_4$ composite electrodes pre-

pared by solvent-route [21]. Because porosity is quite high and does not sensitively vary from one electrode to another, and because ionic conductivity of a composite electrode is generally related to the overall porosity, we think that ionic conductivity is probably a second-rate factor to explain the strong differences in electrochemical performances.

The electrical properties of carbon black polymer composites are generally explained within the framework of classical percolation theory and/or inter-particle tunneling conduction [22]. In this work, the variation of the electrical conductivity versus CB volume fraction for model CB/binder blends and for the corresponding composite $Li_{1.2}V_3O_8$/CB/binder electrodes were typical of the percolation theory [23]. A sharp increase in conductivity was observed for a critical CB volume fraction that corresponds, according to percolation theory, to formation of continuous carbon paths throughout the composite material. The percolation threshold varied according to the nature of the binder and was the same for a model blend (without the active material) and its corresponding electrode. The binder pre-plastification was found to systematically shift the percolation threshold from a CB volume fraction of 4–5% to less than 2%. According to literature, the percolation threshold is usually lower for highly structured carbon black (branched aggregates). Thus, we believe that the lower percolation threshold observed here for pre-plastified electrodes could be related to a more efficient dis-agglomeration of the CB initial aggregates in the presence of the plasticizer. Fig. 3 shows a comparison between the electronic conductivity and the electrochemical performance
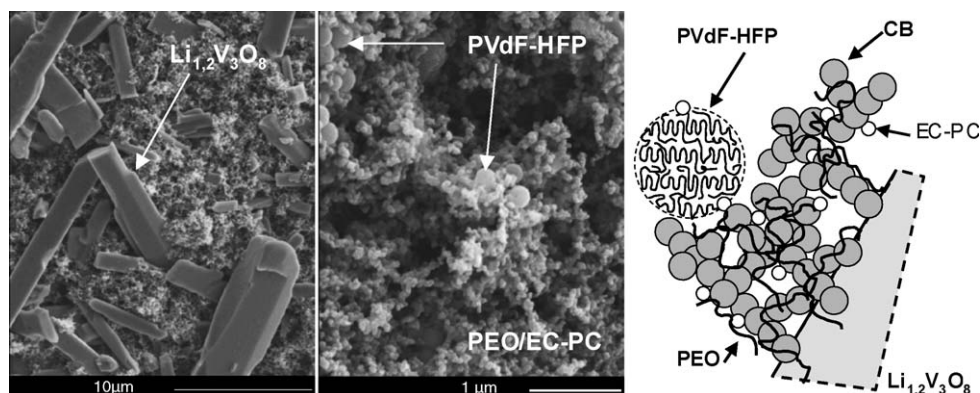

Fig. 2. SEM micrographs of composite electrode E and schematic drawing of its architecture.
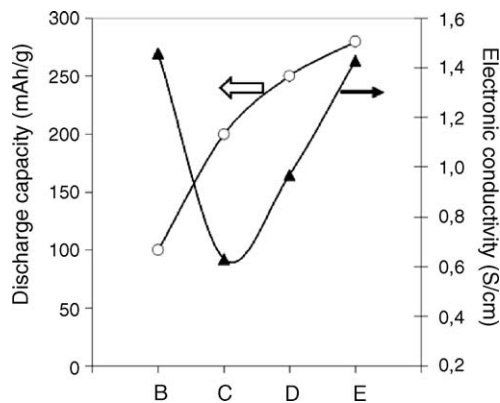
Fig. 3. Electrochemical performance and electrical data. Discharge capacity at room temperature for different cells made with composite electrodes B–E, and the corresponding electronic conductivity.

of the corresponding electrodes. Except for composite B, the capacity variations follow the electronic conductivity variations. Results for composite B suggest, however, that the electronic conductivity is not the only parameter that governs the electrode performance.

Complementary information has been obtained from incremental capacity versus voltage curves. Polarization defined as $E_{ox} - E_{red}$, has been measured at the kinetically limiting step (2.6 V) [12]. For composite electrodes prepared with the same active material and studied in the same conditions, a lower polarization means both a low internal resistance of the electrode (i.e. high electronic conductivity) and faster overall interfacial transfer kinetics. The better charge transfer kinetics comes probably from better CB/Li$_{1.2}$V$_3$O$_8$ interface within the composite complex edifice. Fig. 4 compares electrochemical performance with polarization data for composite electrodes B–E. A good correlation is observed. It means that for electrode B the limiting factor is the charge transfer kinetics while for other electrodes it is the electronic conductivity of the electrode. These results indicate that the efficiency of CB/Li$_{1.2}$V$_3$O$_8$ interface appears also as a main

criterion governing the electrode performance. In the case of electrodes C, D and E, the non-limited charge transfer kinetics probably results from the more efficient CB disagglomeration already discussed above. As a matter of fact, a better CB dispersion leads to a larger available surface area, which results in average to more numerous electrical contacts at the CB/Li$_{1.2}$V$_3$O$_8$ interface.

4. Conclusions

The key roles of the polymeric binder in composite electrodes for lithium battery have been emphasized in the case of an active material, Li$_{1.2}$V$_3$O$_8$, which displays an experimental capacity far below the theoretical value when processed with the standard-type composite electrode procedure. A new polymeric binder has been designed based on preplastified PEO with the electrolyte solvent. Well performing electrode, with efficient electronic conduction network, and better CB/Li$_{1.2}$V$_3$O$_8$ interfaces, was achieved from a more homogeneous and efficient CB distribution due to favorable plastified PEO/CB interactions. Optimized composite electrode allowed reaching a specific capacity of 280 mAh g^{-1} instead of 150 mAh g^{-1} at room temperature. The fairly low cycling capacity usually obtained up to now for Li$_{1.2}$V$_3$O$_8$ electrodes was thus not due to kinetic self-limitations of the active material itself, but to inefficient environment in the electrode.
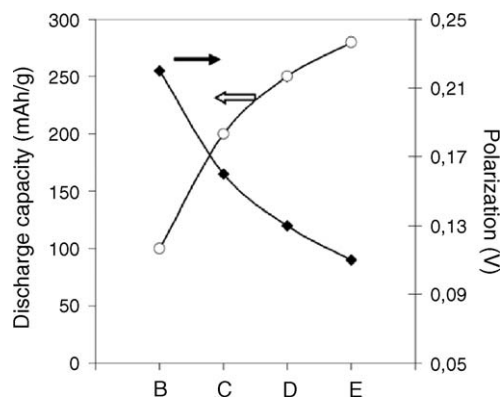
Fig. 4. Electrochemical performance and polarization data. Discharge capacity at room temperature for different cells made with composite electrodes B–E, and the corresponding polarization, defined as $E_{ox} - E_{red}$, measured at 2.6 V.

References

[1] M. Armand, Solid State Ionics 69 (1994) 309.
[2] J.M. Tarascon, A.S. Gozdz, C. Schmutz, F. Shokoohi, P.C. Warren, Solid State Ionics 86–88 (1996) 49.
[3] N.S. Choi, Y.G. Lee, J.K. Park, J. Power Sources 112 (2002) 61.
[4] S.S. Zhang, T.R. Jow, J. Power Sources 109 (2002) 422.
[5] M. Manickam, M. Takata, Electrochim. Acta 48 (2003) 957.
[6] J. Drofenik, M. Gaberscek, R. Dominko, F.W. Poulsen, M. Mogensen, S. Pejovnik, J. Jamnik, Electrochim. Acta 48 (2003) 883.
[7] S. Panero, M. Pasquali, G. Pistoia, J. Electrochem. Soc. 130 (1983) 1225.
[8] F. Bonino, M. Ottaviani, B. Scrosati, G. Pistoia, J. Electrochem. Soc. 135 (1988) 12.
[9] Y. Geronov, B. Puresheva, R.V. Moshtev, P. Zlatilova, T. Kosev, Z. Stoynov, G. Pistoia, M. Pasquali, J. Electrochem. Soc. 137 (1990) 3338.
[10] K. West, B. Zachau-Christiansen, S. Skaarup, Y. Saidi, J. Barker, I.I. Olsen, R. Pynenburg, R. Koksbang, J. Electrochem. Soc. 143 (1996) 820.
[11] D. Guy, B. Lestriez, D. Guyomard, Adv. Mater. 16 (2004) 553.

[12] D. Guy, B. Lestriez, R. Bouchet, V. Gaudefroy, D. Guyomard, Electrochem. Solid-State Lett. 8 (2005) A17.

[13] R. Dominko, M. Gaberscek, J. Drofenik, M. Bele, S. Pejovnik, Electrochem. Solid-State Lett. 4 (2001) 187.

[14] J.K. Hong, J.H. Lee, S.M. Oh, J. Power Sources 111 (2002) 90.

[15] J.L. Leblanc, Prog. Polym. Sci. 27 (2002) 627.

[16] P. Bezot, C. Hesse-Bezot, R. Rousset, C. Diraison, Colloid. Surf. A 97 (1995) 53.

[17] R.W.A. Franco, J.P. Donoso, C.J. Magon, C.B. Rodella, A.O. Florentino, M.J. Saeki, J.M. Pernaut, A.L. de Oliveira, Solid State Ionics 149 (1998) 113.

[18] J.M. Pernaut, G. Goulart, J. Power Sources 55 (1995) 93.

[19] S. Jouanneau, A. Le Gal La Salle, A. Verbaere, D. Guyomard, M. Deschamps, S. Lascaud, Solid State Ionics, in press.

[20] F. Leroux, D. Guyomard, Y. Piffard, Solid State Ionics 80 (1995) 30.

[21] M.G. Lazarraga, S. Mandal, J. Ibanez, J.M. Amarilla, J.M. Rojo, J. Power Sources 115 (2003) 315.

[22] I. Balberg, Carbon 40 (2002) 139.

[23] D. Guy, B. Lestriez, R. Bouchet, V. Gaudefroy, D. Guyomard, Ionics 10 (2004) 443.